TELKOMNIKA, Vol.17, No.6, December 2019, pp.3218~3225
ISSN: 1693-6930, accredited First Grade by Kemenristekdikti, Decree No: 21/E/KPT/2018
DOI: 10.12928/TELKOMNIKA.v17i6.13220

Automatic image slice marking propagation on segmentation of dental CBCT

Agus Zainal Arifin*[1], Evan Tanuwijaya[2], Baskoro Nugroho[3], Arif Mudi Priyatno[4], Rarasmaya Indraswari[5], Eha Renwi Astuti[6], Dini Adni Navastara[7]
[1,2,3,4,5,7]Department of Informatics, Faculty of Information and Communication Technology, Institut Teknologi Sepuluh Nopember (ITS), Surabaya, Indonesia
[6]Department of Dentomaxillofacial Radiology, Faculty of Dental Medicine, Universitas Airlangga, Surabaya, Indonesia
*Corresponding author, e-mail: agusza@cs.its.ac.id[*1], evantanuwijaya.18051@mhs.its.ac.id[2], baskoro.18051@mhs.its.ac.id[3], arif.18051@mhs.its.ac.id[4], rarasmaya16@mhs.if.its.ac.id[5], eharenwi@gmail.com[6], dini_navastara@if.its.ac.id[7]

Abstract

Cone Beam Computed Tomography (CBCT) is a radiographic technique that has been commonly used to help doctors provide more detailed information for further examination. Teeth segmentation on CBCT image has many challenges such as low contrast, blurred teeth boundary and irregular contour of the teeth. In addition, because the CBCT produces a lot of slices, in which the neighboring slices have related information, the semi-automatic image segmentation method, that needs manual marking from the user, becomes exhaustive and inefficient. In this research, we propose an automatic image slice marking propagation on segmentation of dental CBCT. The segmentation result of the first slice will be propagated as the marker for the segmentation of the next slices. The experimental results show that the proposed method is successful in segmenting the teeth on CBCT images with the value of Misclassification Error (ME) and Relative Foreground Area Error (RAE) of 0.112 and 0.478, respectively.

Keywords*: automatic segmentation, dental CBCT, hierarchical clustering, mean-shift, morphology.*

1. Introduction

Cone-beam computed tomography (CBCT) is a radiographic technique that has been commonly used in various applications [1-3]. CBCT provides information in the form of three-dimensional (3D) images. This is an advantage over two-dimensional (2D) panoramic. The 3D image provides more detailed information that can be used for further analysis and examinations. Therefore, CBCT has been widely used for examination rather than panoramic teeth [4-10].

CBCT can be used to help orthodontic surgery [11], by segmenting the bone or teeth. Teeth segmentation is the most important part of the procedure and it is aided by the computer. The results of the computer-aided segmentation can provide feature information about the differences between dental tissues and others. This can be used in the application of dental diagnosis, human identification, dental care, and so on. However, CBCT image usually has low contrast, blurred and irregular tooth borders [12-14]. The three-dimensional (3D) CBCT image can be sliced into several two-dimensional (2D) images. Each 2D slice has information that related to the neighboring slices. However, the teeth topology in each slice is usually different. Those problems provide challenges for the teeth segmentation on CBCT image [15-17].

Research on CBCT image segmentation methods has been carried out. Broadly speaking, the segmentation method can be classified into 3 classes namely manual, semi-automatic and automatic segmentation method [18]. In general, the automatic segmentation methods can be classified further into several classes, which are edge-based, threshold, hybrid, and so on. Wang, et al. [19] conducted research about segmentation on CBCT image using an optimal threshold. The optimal threshold is obtained from the information of first grayscale slice and the merging of gradient value across the slices. Naumovich, et al. [20] segment the teeth and jaws on the CBCT image by using a watershed transformation. The research cut CBCT into several slices before segmentation process is

Received May 27, 2019; Revised July 2, 2019; Accepted July 18, 2019

carried out. However, the research imposes the same treatment in each slice for the segmentation process, so that it does not pay attention to the information contained in each slice. In addition, using semi-automatic image segmentation method becomes exhaustive and inefficient because the CBCT image produces a lot of slices and the method needs the user to mark the teeth on each slice to provide information for the segmentation algorithm.

In this research, we propose an automatic image slice marking propagation on segmentation of dental CBCT. Marker from the segmentation result of the first slice will be propagated as the information for the segmentation of next slices, therefore the relationship between each slice is not ignored. The proposed method performs semi-automatic image segmentation on several slices, in which the user needs to mark the segmentation object to provide the information needed for the segmentation algorithm and use the segmentation result to segment other slices automatically. Using the proposed method, the CBCT image segmentation process can be more effective, because it integrates information from the user for the segmentation process, and becomes more efficient because it only needs to mark several slices.

2. Research Method

In this research, we propose a strategy for segmenting teeth on CBCT images automatically according to Figure 1. Every slice in CBCT images will be inserted starting from the first to ninety pieces. The inputted image will be split into regions, and the marking process is the process of labeling the regions as an object or background.

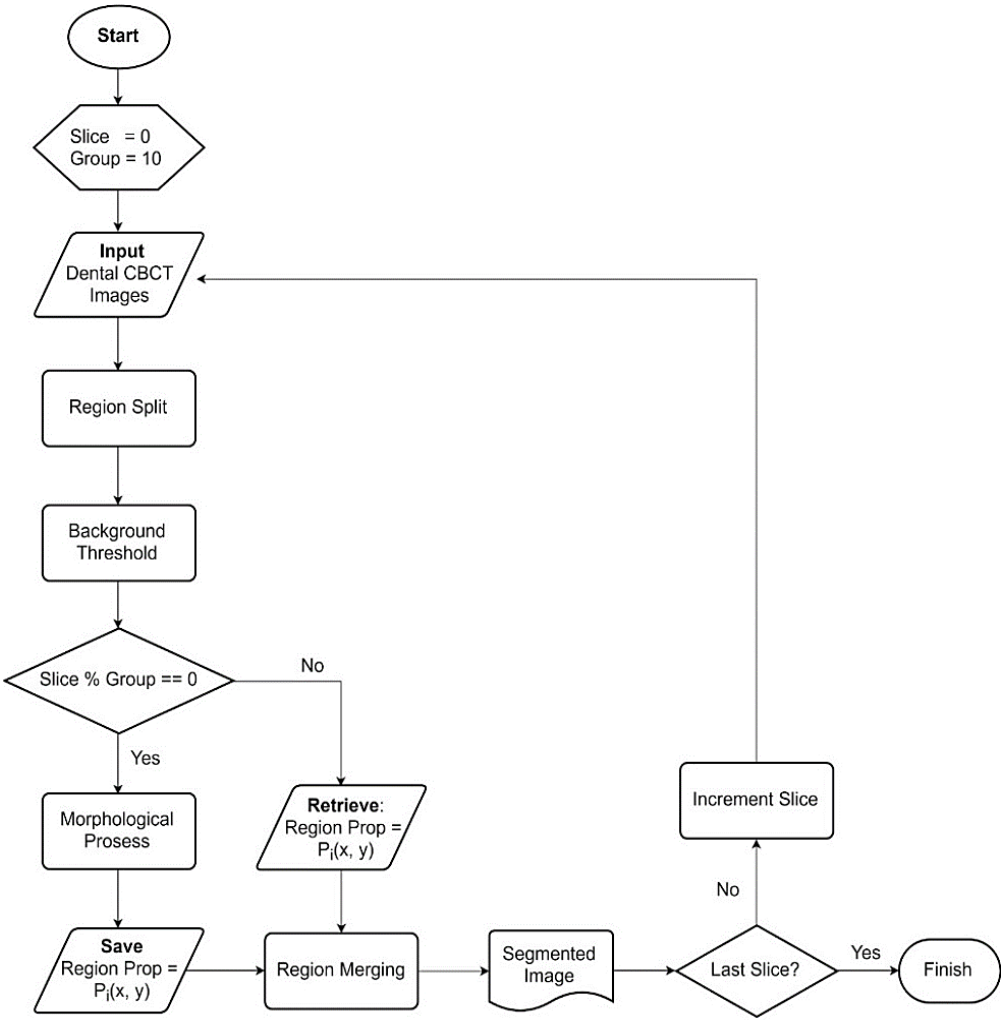

Figure 1. The algorithm of the proposed method

The marking process consists of background threshold, morphological process, and the property regions of morphological results. The morphology process will be carried out per group where one group consists of 10 CBCT images. So that one group only does the morphological process once then the result of the region property will be used on the next nine images. The region properties obtained will be used as the object marker. After that, region merging will be done to group regions that have not been labeled as objects or backgrounds. The result of region merging is the image of teeth that have been segmented. For this research, we used Matlab software in the process.

2.1. Dataset

The data used in this research is Dental CBCT (Cone-Beam Computed Tomography) data taken from the scans of the human jaw. This data was obtained from the Dental and Oral Hospital, Airlangga University (RSGM UNAIR). Every data obtained has a ground truth that has been confirmed by radiological experts so that the accuracy of the proposed method can be calculated. This data set is 3D data, which is then sliced according to the axial plane and result in 2D images as shown in Figure 2. The result of the slicing process is 200 images with the size of 266x266 pixels each [21].

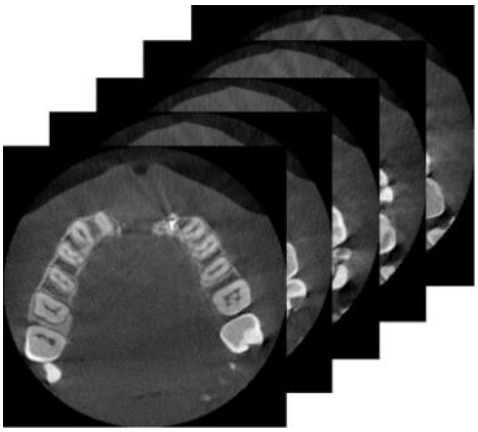

Figure 2. Dental CBCT

2.2. Region Splitting

The first stage in this segmentation process is the region splitting where CBCT images are separated into several regions. The algorithm that researchers use to do this region splitting is mean-shift clustering [22]. This algorithm divides CBCT images into cluster regions according to color similarity. The mean-shift that the researchers used was a mean-shift by the Edison System [23]. The mean-shift used has several input parameters in the form of spatial bandwidth, bandwidth range, and minimum area region. The values of each parameter are 7, 10 and 11. The results of the splitting region with the mean-shift algorithm are images that have been divided into cluster regions, which can be seen in Figure 3.

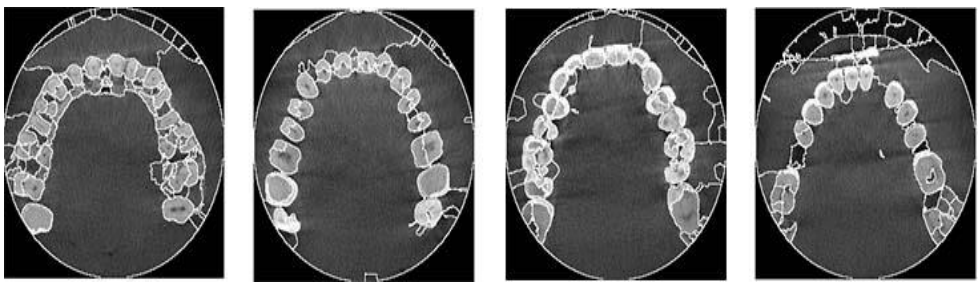

Figure 3. Region splitting

2.3. Marking Process

An image consists of objects and non-objects (background). In the segmentation process, it is necessary to know the object's boundaries to separate objects from the background. In the region splitting process, CBCT images are divided into several cluster regions. The cluster will later be labeled as an object or background. This marking process aims to mark these clusters as objects or backgrounds. Therefore, the researcher concludes that image (I) of the results of this marking process will consist of the object (O), background (B), and non-marked cluster (C) according to (1).

$$I = \{O, B, C\} \quad (1)$$

To mark the tooth as objects, the initial image is used before the region splitting. This marking process is carried out every 10 slices of data starting data pieces from the 10th, 20th, and up to the 90th slice in to speed up the segmentation process with large amounts of data slices. The marking process of the 10th slice will be used as a marker for the next 9 slices. For the 20th slice, the re-marking process will be carried out, and the next 9 slices will use the marking information from the 20th slice.

The first stage of the marking process is the background threshold. The threshold value used is the average threshold value of all CBCT image entries with the algorithm [18] so that the gray color below the threshold will be considered as background and omitted to 0. For the value above the threshold, the gray color is changed to 1. The result of the background threshold is then inserted into the filter process to remove background noise that is still remaining. The remaining background noise like small dots still remains in the image. To remove the noise, median filtering is performed three times. In Figure 4, the left image shows the image before the median filtering process was done, and the right image shows the result from the median filtering.

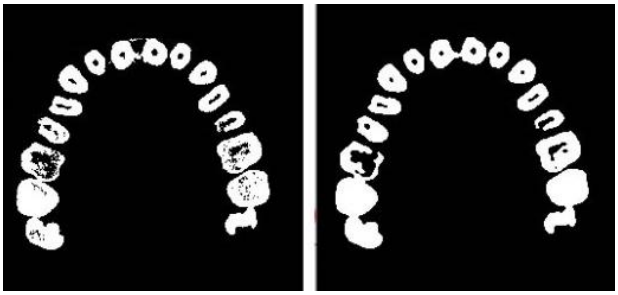

Figure 4. The result of the median filtering

The next step is the morphological process. Morphology used is a circle. The circle model is used because the shape of human teeth in CBCT images is assumed to be like a circle. The results of the morphology are taken from the property region of each circle obtained. Region property obtained is a centroid, major axis length, minor axis length. To find the diameter *D* of a circle, the researcher uses the following (2).

$$\mathrm{D} = \frac{(\text{major axis length}/2)\times(\text{minor axis length}/2)}{2} \quad (2)$$

The major axis length and the minor axis length are values of the property region. The value of the major axis length and minor axis length is divided by 2 to shrink the object markers so that the background is not marked. The results of the marking process can be seen in Figure 5. In the results of the property regions, the researcher gets circles that indicate the position of the object like Figure 5 (b). The circles are the entire coordinate of the object so the researcher takes several coordinates (x, y) by drawing a straight line in the middle of each circle, so that all the coordinates of the object are obtained. For the background marking process is done by taking a number of coordinates that are far outside each circle. So that there

is a cluster region that has been labeled as object O consist of N cluster object O_i like (3) and background B consist of M cluster background B_i like (4).

$$O = \{O_i\}_{i=1,\ldots,N} \quad (3)$$

$$B = \{B_i\}_{i=1,\ldots,M} \quad (4)$$

(a) (b)

Figure 5. (a) Result of background threshold and median filter, and (b) its marker

2.4. Region Merging

In the region merging phase, the hierarchical clustering method we use was modified, which was modified at the distance measurement [18]. Distance measurement in hierarchical clustering is modified by observing inter-class and intra-class distances. This modified hierarchical clustering method requires several input parameters. These parameters are the location of the object pixels, which is marked in the previous process, location of the background pixels, initial image, and the result of region splitting process. The process carried out to the non-labeled regions. These non-labeled regions will be counted with the region that has been labeled from the results of the marking process. Regions that are not labeled will be calculated inter-class and intra-class with the region of the cluster object and background. The results of calculating the distance between objects and background will be compared. The lowest distance, whether it's an object or background will be labeled as the cluster. So, the results of the region splitting will merge into clusters that have been labeled and produce a segmented image. Figure 6 is the result of region merging, which is a segmented image.

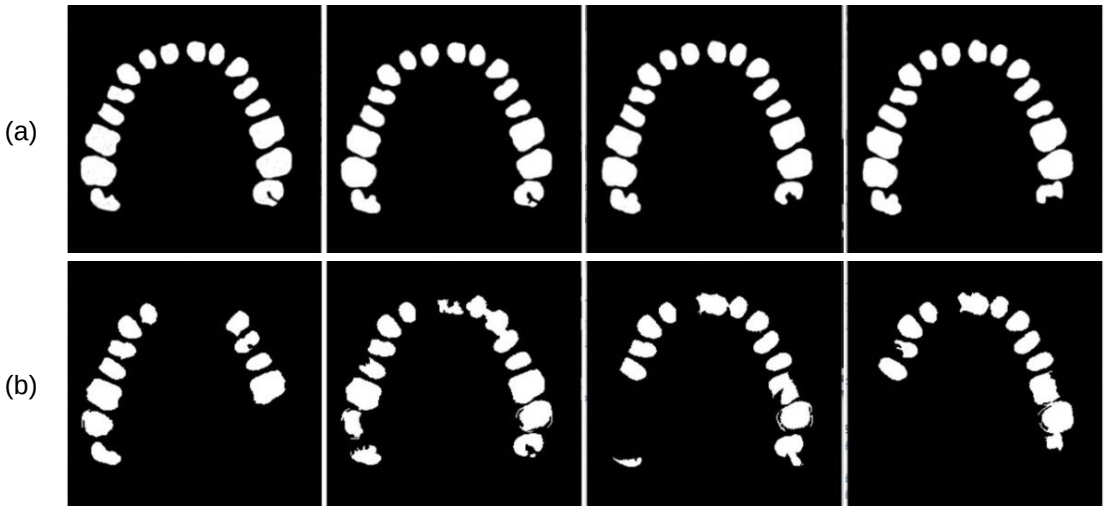

(a)

(b)

Figure 6. (a) Ground truth images 1st – 4th slices and (b) segmentation result 1st – 4th slices

3. Result and Discussion

The results of the automatic tooth segmentation research on CBCT data will be compared with the existing automatic methods, namely OTSU [24] and HCA [25]. To evaluate this proposed method, researchers used Misclassification Error (ME) and Relative Foreground Area Error (RAE). The ME value measures the object and background pixels that are wrongly classified. RAE serves to measure the difference in area between segmented objects and ground truth. ME has a calculation equation like (5).

$$\mathrm{ME} = 1 - \frac{|\mathrm{O_g} \cap \mathrm{O_r}| + |\mathrm{B_g} \cap \mathrm{B_r}|}{|\mathrm{O_g} \cup \mathrm{B_g}|} \quad (5)$$

The calculation process of Misclassification error (ME) uses the total number of error probabilities (1) minus the number of truths that were successfully performed. The process of calculating the amount of truth is done by dividing the number of pixels that are correctly classified divided by the total pixel image. The truth of the total pixel is calculated by summing the total similarity pixels of the ground truth (Og) object and the total pixel segmentation result (Or) and the total pixel similarity to the background image (Bg) and the total pixel background of the segmentation (Br). The smaller ME results, the better segmentation results. A calculation formula for RAE is explained in (6).

$$\mathrm{RAE} = \begin{cases} \frac{\mathrm{A_g} - \mathrm{A_r}}{\mathrm{A_g}} & \text{if } \mathrm{A_r} < \mathrm{A_g} \\ \frac{\mathrm{A_r} - \mathrm{A_g}}{\mathrm{A_r}} & \text{if } \mathrm{A_r} \geq \mathrm{A_g} \end{cases} \quad (6)$$

Where Ag is an area of the image of ground truth, Ar is an area of image segmentation results. The smaller the RAE value, the more similar the results of segmentation with ground truth so that it produces good segmentation results. In Table 1 shows the results of the trial of the proposed method with OTSU and HCA. The results obtained stated that the ME and MAE mean values of the proposed method were 0.112 and 0.478. The OTSU method obtained ME and MAE averages of 0.410 and 0.657 and the HCA method averaged ME and MAE of 0.398 and 0.719. It can be concluded that the proposed method has a better level of accuracy compared to automatic segmentation methods such as OTSU and HCA.

The compared methods perform image segmentation using threshold value (automatically) and do not pay attention to the neighborhood value and 3D information of CBCT image. This causes the background that has an intensity value above the threshold to be classified as an object and the objects that has an intensity value below the threshold to be classified as background. The error comparison result on Table 1 shows that the proposed method gives more effective segmentation results, proven by the smaller error values, than the automatic segmentation methods because the proposed method integrates information from the user for the segmentation process.

Marking objects automatically using morphology and property regions can detect teeth on CBCT images that are shaped like circles. However, as shown in Figure 6, the region merging process cannot detect all the teeth because some teeth region has a more similar intensity to the background. This caused segmentation error and further analysis about more accurate region merging method can be performed.

Table 1. Comparison Results of the Proposed Method

No	CBCT Data	Proposed Method		OTSU		HCA	
		ME	MAE	ME	MAE	ME	MAE
1	A	0.112	0.309	0.340	0.544	0.360	0.621
2	B	0.097	0.423	0.434	0.729	0.384	0.729
3	C	0.122	0.662	0.521	0.934	0.418	0.810
4	D	0.074	0.458	0.313	0.530	0.365	0.778
5	E	0.088	0.572	0.491	0.790	0.483	0.843
6	F	0.130	0.529	0.416	0.619	0.384	0.661
7	G	0.160	0.392	0.353	0.449	0.393	0.590
Average		0.112	0.478	0.410	0.657	0.398	0.719

4. Conclusion

In this research, we propose a strategy in segmenting teeth automatically. This research used dental CBCT data taken from several patients from the RSGM UNAIR hospital. The proposed method has several stages, which are region splitting using the mean-shift algorithm, marking using morphology and property regions, and region merging using hierarchical clustering algorithm. The results obtained from the proposed method have lower error values than the existing automatic segmentation method, which are the ME value with an average of 0.112 and the MAE value with an average of 0.478. The experimental results show that the proposed method can automatically segment the CBCT data by paying attention to its 3D information. The effectiveness of the proposed method is indicated by the low error rate compared to the other methods. Further research about the parameters or algorithms for conducting region splitting and region merging process is needed to produce a more effective and efficient result.

References

[1] Studebaker B, Hollender L, Mancl L, Johnson JD, Paranjpe A, The Incidence of Second Mesiobuccal Canals Located in Maxillary Molars with the Aid of Cone-beam Computed Tomography. *Journal of endodontics*. 2018; 44(4): 565–570.

[2] Patel S, Dawood A, Ford TP, Whaites E. The potential applications of cone beam computed tomography in the management of endodontic problems. *International endodontic journal*. 2007; 40(10): 818–830.

[3] John GP, Joy TE, Mathew J, Kumar VR. Applications of cone beam computed tomography for a prosthodontist. *The Journal of the Indian Prosthodontic Society*. 2016; 16(1): 3.

[4] Lee RJ, Pi S, Park J, Nelson G, Hatcher D, Oberoi S. Three-dimensional evaluation of root position at the reset appointment without radiographs: a proof-of-concept study. *Progress in orthodontics*. 2018; 19(1): 15.

[5] Kumar M, Shanavas M, Sidappa A, Kiran M. Cone beam computed tomography-know its secrets. *Journal of international oral health: JIOH*. 2015; 7(2): 64–68.

[6] Ketabi AR, Ketabi S, Nabli MB, Lauer HC, Brenner M. Detection and measurements of apical lesions in the upper jaw by cone beam computed tomography and panoramic radiography as a function of cortical bone thickness. *Clinical oral investigations*. 2019; 22: 1-7.

[7] Aminoshariae A, Kulild JC, Syed A. Cone-beam Computed Tomography Compared with Intraoral Radiographic Lesions in Endodontic Outcome Studies: A Systematic Review. *Journal of endodontics*. 2018; 44(11): 1626–1631.

[8] Patel S, Durack C, Abella F, Shemesh H, Roig M, Lemberg K. Cone beam computed tomography in Endodontics–a review. *International endodontic journal*. 2015; 48(1): 3-15.

[9] Rodríguez G, Abella F, Durán-Sindreu F, Patel S, Roig M. Influence of Cone-beam Computed Tomography in Clinical Decision Making among Specialists. *Journal of endodontics*. 2017; 43(2): 194–199.

[10] Rodríguez G, Patel S, Durán-Sindreu F, Roig M, Abella F. Influence of Cone-beam Computed Tomography on Endodontic Retreatment Strategies among General Dental Practitioners and Endodontists. *Journal of endodontics.* 2017; 43(9): 1433–1437.

[11] Nilsson J, Richards RG, Thor A, Kamer L. Virtual bite registration using intraoral digital scanning, CT and CBCT: In vitro evaluation of a new method and its implication for orthognathic surgery. *Journal of Cranio-Maxillofacial Surgery*. 2016; 44(9): 1194–1200.

[12] Kakehbaraei S, Seyedarabi H, Zenouz AT. Dental Segmentation in Cone-beam Computed Tomography Images Using Watershed and Morphology Operators. *Journal of medical signals and sensors.* 2018; 8(2): 119–124.

[13] Lv J, Wang F, Xu L, Ma Z, Yang B. A segmentation method of bagged green apple image. *Scientia horticulturae.* 2019; 246: 411–417.

[14] Fan Y, Beare R, Matthews H, Schneider P, Kilpatrick N, Clement J, Claes P, Penington A, Adamson C. Marker-based watershed transform method for fully automatic mandibular segmentation from CBCT images. *Dentomaxillofacial Radiology.* 2019; 48(2): 20180261.

[15] Gao H, Chae O. Individual tooth segmentation from CT images using level set method with shape and intensity prior. *Pattern Recognition*. 2010; 43(7): 2406-2417.

[16] Xia Z, Gan Y, Chang L, Xiong J, Zhao Q. Individual tooth segmentation from CT images scanned with contacts of maxillary and mandible teeth. *Computer methods and programs in biomedicine*. 2017; 138:1-2.

[17] Gan Y, Xia Z, Xiong J, Li G, Zhao Q. Tooth and Alveolar Bone Segmentation From Dental Computed Tomography Images. *IEEE journal of biomedical and health informatics*. 2017; 22(1): 196-204.

[18] Arifin AZ, Arifiani S, Fariza A, Navastara DA, Indraswari R. *Hierarchical Clustering Linkage for Region Merging in Interactive Image Segmentation on Dental Cone Beam Computed Tomography*. IEEE International Conference on Applied Information Technology and Innovation (ICAITI). 2018: 124–128.
[19] Wang L, Li JP, Ge ZP, Li G. CBCT image based segmentation method for tooth pulp cavity region extraction. *Dentomaxillofacial Radiology*. 2018; 48(2): 20180236.
[20] Naumovich SS, Naumovich SA, Goncharenko VG. Three-dimensional reconstruction of teeth and jaws based on segmentation of CT images using watershed transformation. *Dentomaxillofacial Radiology.* 2015; 44(4): 1–6.
[21] Indraswari R, Kurita T, Arifin AZ, Suciati N, Astuti ER, Navastara DA. *3D Region Merging for Segmentation of Teeth on Cone-Beam Computed Tomography Images*. IEEE Joint 10th International Conference on Soft Computing and Intelligent Systems (SCIS) and 19th International Symposium on Advanced Intelligent Systems (ISIS). 2018: 341-345.
[22] Cheng Y. Mean Shift, Mode Seeking and Clustering. *IEEE transactions on pattern analysis and machine intelligence.* 1995; 17(8): 790–799.
[23] Comaniciu D, Meer P. Mean Shift: A Robust Approach Toward Feature Space Analysis. 2002; 24(5): 603–619.
[24] Otsu N. A Threshold Selection Method from Gray-Level Histograms. *IEEE transactions on systems, man, and cybernetics*. 1979; 20(1): 62–66.
[25] Puspaningrum A, Nur N, Riza OS, Arifin AZ. Image thresholding based on hierarchical clustering analysis and percentile method for tuna image segmentation. *Nusantara Journal of Computers and its Applications*. 2018; 2(1): 1–8.